An Initial Approach to Segmentation and Analysis of Nerve Cells using Ridge Detection

S.J. Richerson[1], A. P. Condurache[2], J. Lohmeyer[3], K. Schultz[1], P. Ganske[1]
[1]Biomedical Engineering Program, Milwaukee School of Engineering, Milwaukee Wisconisn, USA
[2] Institute for Signal Processing, University of Lübeck, Lübeck Germany
[3] Plastic surgery, Hand surgery & Intensive-care Unit, University Hospital of Schleswig-Holstein, Campus Lübeck, Germany

Abstract – **Histological studies of nerve fibers are used by researchers to explore many nerve pathologies and treatments. Manual analysis and interpretation of hundreds of nerve fibers typically seen on one cross-sectional image is hardly possible and therefore, we propose here a semi-automated tool designed specifically for this purpose. Our tool returns automatically a segmentation proposition, which can then be improved by the user, i.e. semi-automatically, if so desired. The segmentation results are analyzed again automatically, to obtain several measures. For the segmentation, ridges of the cells are first enhanced by means of the first eigenvalue of the hessian matrix. Then, a hysteresis-based ridge segmentation returns the outline of the cell, which is used to separate it from the background. During semi-automatic processing, the user has the ability to (1) remove any cells in the histological image that as not desired cells or (2) add any cells not initially detected. To analyze the properties of each individual cell, the size of each cell as well as a measure of wall thickness is calculated. In images of good contrast, where nerve cells are large and well spaced, the automatic cell detection rates are between 90 - 95%. In images with poor contrast with small nerve cells tightly packed together, the cell detection rate is 50-75%.**

Keywords – **Hessian matrix, Semi-automatic segmentation, Ridge detection**

I. INTRODUCTION

Measurements of size and wall thickness of nerve fibers can aid neural researchers in determining the health and development of axons during various experiments. These measurements are difficult to undertake because often images of nerve histology have several hundred nerve fibers that are very small in size. In the analyzed images, the axons show a bright body surrounded by the dark myelin sheath, i.e. similar to a cell body with membrane. In the following we refer, where no confusion is possible, to the axon's body and the myelin sheath as the cell nucleus and cell wall respectively. Clearly, cell-segmentation methods are applicable here. Several methodologies have been developed so far to segment cells.

Methods based on thresholding and edge detection [1-2] only work well if the contrast of the image is excellent. However in most cases, this technique yields broken edges and poor detection in noisy environments. Watershed techniques [3-5] have also been applied to the problem of cell segmentation. If the gradients in the image are large enough, then the background can be easily separated from the foreground, however, often the gradients for small closely spaced nerve cells do not meet this requirement. Finally, several attempts have been made to use a priori knowledge of the shape of the cells to detect cell nuclei and fit contours to the cells [6-9], however, often these techniques segment only a small number of the cells in any image.

In this paper, we present a semi-automatic tool, designed specifically for the analysis of cross-sectional images showing nerve histology. This tool utilizes ridge enhancement [10] to improve the contrast of the myelinated sheath and thus support the segmentation of cells in images that are of poor contrast and contain small closely spaced nerve cells. The segmentation takes place on the enhanced images and makes use of a priori information regarding the connectivity of cells. We have successfully compared our method against global thresholding and watershed-based methods.

II. METHODS

The cross-sectional, stained, histology-images of nerve cell were acquired from microscopes at the University Hospital of Schleswig-Holstein, Campus Lübeck, in Lübeck Germany. The RGB images were transformed to an 8-bit gray-scale image by extracting the red channel of the image. This channel was chosen because it yielded the largest contrast between the background and the cell walls. A typical cross sectional nerve image is given in Fig.1 (a) and (b). In general, images showing large cells whose cells walls do not touch, were termed "good" images (see Fig. 1(a)). Images which contained small cells whose walls were in contact with one another, were termed "poor" images (see Fig. 1(b)). Note that in both cases the intensity of cell nuclei is brighter than the myelin sheath (although this difference is much larger in good images). The myelin sheath is the ring area enclosed by inner and outer contours where the intensity is lower than cell nucleus.

Our tool includes two main steps, i.e., segmentation and analysis. To find an axon, we first segment the myelin sheath. The ring-like structures are then filled by a flood-fill operation to obtain the entire axon. To support the segmentation of the myelin sheath, we process the input image to enhance the ridges (myelin) of the cell using the first eigenvalue of the Hessian matrix. The segmentation is done with hysteresis methods [12]. We obtain thus automatically a segmentation result.

This approach is successful for "good" images as ridges are well defined in this case. However, for "poor" images, this approach yielded fewer segmented cells.

To enhance the segmentation for these "poor" images, a second user-supported segmentation step was added. Once the automatic segmentation is complete, users have the ability to remove cells based on cell size, delete detected non-nerve cells, and add non-detected nerve cells either manually or using a marker-based Watershed Transformation [16].

Once the segmentation is completed, the tool then automatically analyzes the segmented image to determine the number of cells in the image, the diameter of each cell, and the thickness of myelin sheath for each cell.

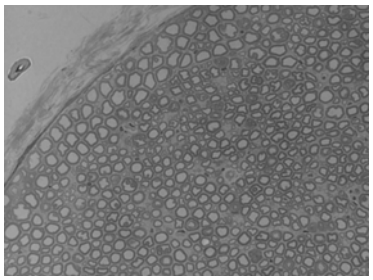

(a)

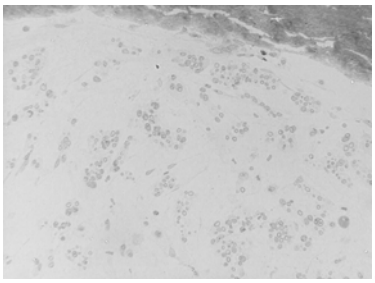

(b)

FIGURE 1: Typical cross-sectional nerve cells. (a) A "good" image: A nerve image that contains large cells with myelin sheaths that do not touch. The intensity difference between the cell nucleus and the myelin sheath is large. (b) A "poor" image: A nerve image that contains small nerve cells with myelin sheaths that touch. The intensity difference between the cell nucleus and the myelin sheath is small.

A: Automatic Segmentation

The automatic segmentation includes ridge enhancement, hysteresis segmentation and removal of non-filled cells. Details of each step are given below.

Ridge Enhancement using the first Eigen value of the Hessian matrix – The Hessian matrix of an image f is a square matrix of second order partial derivatives (see eq. 1.1). This matrix has orthogonal eigenvectors and real eigenvalues. Its first eigenvalue (eq. 1.2) responds to ridges in the image [11]. To further increase the difference between the values of the myelin sheath and the background, we take the exponential of each pixel value. Figure 2 shows the result of ridge enhancement on a "good" image.

$$H = \begin{bmatrix} f_{xx} & f_{xy} \\ f_{yx} & f_{yy} \end{bmatrix} \quad (1.1)$$

$$\lambda_1 = \frac{1}{2}\left[\left(f_{xx} + f_{yy}\right) - \sqrt{\left(f_{xx} + f_{yy}\right)^2 - 4\left(\left(f_{xx} * f_{yy}\right) - \left(f_{xy}^2\right)\right)}\right] \quad (1.2)$$

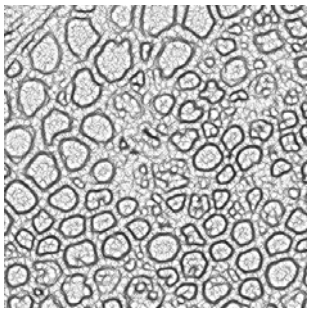

FIGURE 2 Results of the ridge detection algorithm that utilizes the first Eigen value of the Hessian Matrix. Note this is a sub-section of the image found in Figure 1a.

Hysteresis-Based Ridge Segmentation– The image is first segmented by a 'hard' threshold, which yields high confidence ridge pixels. A second threshold operation with a 'weak' threshold, returns then the entire object together with many background pixels. Using prior knowledge with respect to object connectivity, the segmentation is achieved by choosing from among the object pixels selected by the 'weak' threshold only those pixels connected to a high confidence one [12-13]. The connected cell boundaries are then filled.

Removal of Non-filled Cells – Any cell boundaries that were broken and did not fill properly are removed by morphologically opening the image [14]. A disk shaped structuring element with a radius of 3 pixels is used in the opening.

After completion of the automatic segmentation, the segmented image is overlaid on the original image and presented to the user (see Fig. 3(a) and (b)).

B: Semi-automatic processing

If the user is not satisfied with the automatic segmentation, he can manually improve it by: removing falsely-detected cells and adding miss-segmented cells.

Remove cells based on cell size – Users may chose this option and then input the largest and smallest number of pixels that a cell can contain. The program then automatically deletes any detected cells with sizes larger and smaller than the user input.

Deletion of detected non-nerve cells – Users may choose this option and then select segmented cells that are not nerves. These selections will then be removed from the segmented image. During the automatic segmentation, blood vessels and other cell types may be automatically segmented. If the user wants to ignore these during analysis (e.g. in the top left hand corner of Figure 3 is a non-nerve

cell), he/she can delete them. For this purpose, the user has to select manually a seed inside the desired cell. A connected-components analysis [15] finds then all object pixels liked to the seed. These pixels are then removed from the segmentation result.

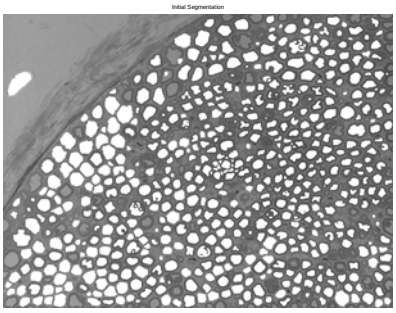

(a)

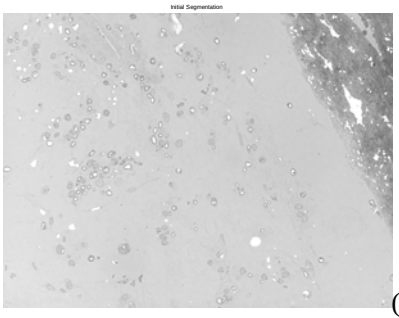

(b)

FIGURE 3: Automatically segmented image overlaid on original image. Automatically segmented pixels appear in white over the gray image (a) Segmentation of good image. (b) Segmentation of poor image.

Addition of non-detected nerve cells – If there are cells not detected by the automatic segmentation, the user is given two options to add cells to the final segmented image. The first choice utilizes a marker-based watershed transformation [16], which works well on cells that have distinctly lower intensity myelin sheaths and higher intensity cell nuclei (this generally occurs in "good" images only). The user selects a local region of the total image and the program automatically computes the watershed transformation for this region. By applying the watershed transform locally, we compensate for the varying-contrast conditions and thus achieve satisfactory results in comparison to a globally applied watershed transform (see Section II). If the gradient is not large enough or the cell fails to segment properly, the users then have the option to draw a line around the cell and choose to add it to the final segmented image. This manual addition is generally not needed in good images, as the watershed transformation segments most cells; however, in poor images, the gradient is usually too small for the watershed transformation to work properly.

Once the user has completed any user-defined segmentation, he/she can choose to analyze the image.

C. Analysis

Determine number of cells in image – Each connected component (cell) is labeled in the image, using the method described in Reference [17]. The total number of labeled cells is then output to the user

Determine size of each cell in image –A generalized Hough transformation [15] is used to fit an ellipse to each labeled cell. The measurement of the minor axis of the ellipse (in pixels) is then calculated and saved with the cell label.

Determine thickness of myelin sheath – We measure the thickness of the myelin sheath relative the cell area. For this purpose, each segmented cell is cropped out of the original image. The corresponding gray-levels belong now to one of two possible classes: axon body or myelin sheath. The class labels for each pixel are then determined by thresholding [18]. The number of myelin-sheath-pixels is divided by the total number of pixels to calculate the fraction of the cell surface that is myelin. This metric (expressed as a percentage) is then saved with the length of the minor axis calculated previously.

II. EXPERIMENTAL RESULTS AND DISCUSSION

In this section, experimental results of this ridge based algorithm are compared to two other algorithms. First, a percentile based method is used. This method determines the histogram of the image and then uses the cell myelin intensity to determine the percentile to which that intensity belongs. The entire image is the segmented based on the percentile determined. The holes in the image are then filled. The second algorithm used for comparison is a marker based watershed algorithm [15] that is performed globally on the entire image. This method computes a segmentation function, and then determines the foreground and background markers. The segmentation function is then modified so that it only has minima at the foreground and background marker locations. The watershed transform is then applied to the modified segmentation function.

Comparisons can be seen in Fig. 4(a), 4(b), and 4(c). The percentile based method (see Fig. 4(a)) segments many cells, however the process fails to find any cells in the lower left hand corner, and there are several cells in the center and upper right hand corner of the image that are connected and thus would be counted as one cell. The watershed methodology (see Fig. 4(b)) segments more cells than the percentile-based method, but also segments background areas as a detected cell in areas of low contrast (lower left hand side). Additionally, this segmentation only detects the interior of the cell and fails to detect the myelin, making it difficult to measure the thickness of the myelin. The ridge based algorithm presented here (see Fig. 4(c)) segments many more cells

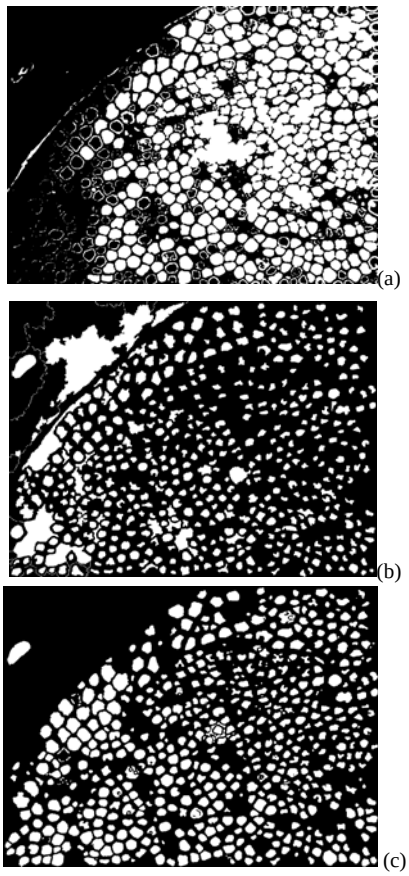

FIGURE 4: Comparison of Percentile Based Segmentation and Ridge Based Segmentation on image shown in Figure 1a. (a)Segmentation done using the percentile based method (20%). (b) Segmentation using a marker based watershed transformation. (c)Segmentation using the ridge based method presented in this paper.

accurately, including the myelin sheath, especially in the lower left hand corner (the lowest contrast area in the picture). With additional user-defined segmentation cells that are not nerve cells can be deleted and additional cells can be added to the figure.

As there is still no ground-truth available for axon segmentation, we have evaluated our algorithms visually on several (i.e. twenty) nerve images. The evaluation was done by trained personnel under the supervision of the third author.

Our method represents a clear improvement over manual segmentation and other non-specific methods used until now to segment and analyze axons in cross-sectional images. We obtain reproducible results and better accuracy.

IV. CONCLUSION AND FUTURE WORK

We have proposed a novel tool to be used in neural cell image segmentation that utilizes a ridge based segmentation algorithm. As this tool is dedicated to medical research, time constrains are less important than the degree of accuracy to which the cells are segmented. Therefore, user input in addition to the automatic segmentation yields a higher level of accuracy than allowed in any other automatic segmentation method. The automatic segmentation portion of this tool works extremely well on images with large cells spaced fairly far apart. In images with small closely spaced cells, the automatic segmentation performs fairly, but results can be improved by the user with the manual segmentation step. This tool has been developed and refined using approximately twenty different histological images.

In further work, this tool will be validated by medical personnel using additional images. We intend to construct a data-basis containing the ground truth for several images, which we will make public such as to support further research in the field. We also look to further improve the automatic segmentation, mainly by superior pre-processing.

V. REFERENCES

[1]. Mussio, P., Pietrogrande, R., Bottoni,P., Dell'Oca, M., Arosio, E., and Sartirana, E., Automatic cell count in digital images of liver tissue sections. In: Computer-Based Med. Syst. Fourth Ann. IEEE Symposium 152**,** 1991.

[2]. Wu, H.S, Berba, J.,Gil, J., Iterative thresholding for segmentation of cells from noisy images, Journal of Microscopy, 197(3), 296–304, 2002.

[3]. Costa, A.F., Mascarenhas, N.D., and De Andrade Netto, M.L., Cell nuclei segmentation in noisy images using morphological watersheds, Proc. SPIE vol. 3164, pp. 314-324, 1997.

[4]. Gauch, J.M., Image segmentation and analysis via multiscale gradientwatershed hierarchies , IEEE Transactions on Image Processing. Vol. 8, no.1, pp. 69-79. Jan. 1999.

[5]. Wang, Y.Y., Sun, Y.N., Lin, C.C.K., Ju, M.S., Nerve Cell Segmentation via Multi-Scale Gradient Watershed Hierarchies, Engineering in Medicine and Biology Society, 2006.

[6]. Fok, Y-L., Chan, J., Chin, R. T. Automated analysis of nerve-cell images using active contour models, IEEE transactions on medical imaging, vol. 15, no. 3, p. 353-368, 1996.

[7]. Bamford, P., and Lovell, B., Unsupervised cell nucleus segmentation with active contours, Signal Processing, 71(2), 203-213, 1998.

[8]. Wu, H.-S., Barba, J., Gil, J.A., parametric fitting algorithm for segmentation of cell images, IEEE Transactions on Biomedical Engineering. Vol. 45, no. 3, pp. 400-407. Mar. 1998

[9]. Mouroutis, T., Roberts, S.J. and Bharath, A.A., Robust cell nuclei segmentation using statistical modeling, Bioimaging, vol. 6, no. 2, pp. 79-91, 1998.

[10]. Maintz, J.B.A., Van Den Elsen, P.A., Viergever, M.A., Evaluation of Ridge Seeking Operators for Multimodality Medical Image Matching, IEEE transactions on pattern analysis and machine intelligence, vol. 18, n◦4, pp. 353-365, 1996.

[11]. Barth,E., Caelli,T., Zetzche, C., Image encoding, labeling, and reconstruction from differential geometry, Graphical Model and Image Processing, 55(6), 428-446, 1993.

[12]. Condurache, P. A., Aach,T, Vessel Segmentation in Angiograms using Hysteresis Thresholding In: Proceedings of the Ninth IAPR conference on Machine Vision Applications 2005, Tsukuba Science City, Japan May 16-18,269-272, 2005.

[13]. Canny, J., A computational approach to edge detection, *IEEE TPAMI*, vol.8, no6, 1986.

[14]. Haralick, R., and Shapiro, L., Computer and Robot Vision, Vol. 1, Addison-Wesley Publishing Company,174 – 185, 1992.

[15]. Gonzalez, R.C. and Woods, R.E., Digital Image Processing, Prentice Hall, 1993.

[16]. Beucher, S., Segmentation Tools in Mathematical Morphology, HPRCV97, Chapter II, 1997.

[17]. Haralick, R., and Shapiro, L., Computer and Robot Vision, Vol. 1, Addison-Wesley Publishing Company, 28 – 48, 1992.

[18]. Otsu N., A threshold selection method from gray-level histograms, IEEE TSMC vol. 9, no.1, pp. 62-66, 1979